JACS Au
AN OPEN ACCESS JOURNAL OF THE AMERICAN CHEMICAL SOCIETY

pubs.acs.org/jacsau
Article

Programmable Single-Stranded Circular Antisense Oligonucleotides for Multitarget Gene Therapy

Published as part of the JACS Au special issue "DNA Nanotechnology for Optoelectronics and Biomedicine".

Yufan Pan,[▽] Xin Li,[▽] Chenyou Zhu, Mingyan Wang, Yuanyuan Wu, Rui Xu, Jun Wu, Ruofan Chen, Yifan Jiang, Baolei Tian, Yuanchen Dong,* and Dongsheng Liu*

Cite This: JACS Au 2025, 5, 3555−3564

Read Online

ACCESS | Metrics & More | Article Recommendations | Supporting Information

ABSTRACT: Oligonucleotide therapeutics, especially antisense oligonucleotides (ASOs), provide promising treatments for various diseases, with combinatorial ASO therapy increasing the efficacy. However, challenges persist in enhancing stability and ensuring precise delivery. Here, we proposed the use of single-stranded circular ASOs (circASOs) for the cosilence of multiple genes, which was demonstrated with universality. Notably, unmodified circASOs achieved a similar silencing efficiency compared to chemically modified ASOs. Multitargeted circASOs were also designed for simultaneous silencing of different genes, showing prolonged and higher gene silencing due to their high biostability. Furthermore, the circASO is compatible with various chemical modifications, which could further enhance the circASO functionality. This programmable circular ASO platform provides a versatile tool for designing multifunctional nucleic acid medicines for gene therapy.

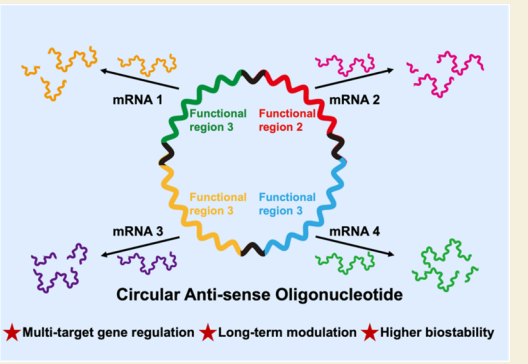

KEYWORDS: *antisense oligonucleotides, chemical modification, circular DNA, gene regulation, multitarget therapy*

INTRODUCTION

Oligonucleotide therapeutics have emerged as a promising platform for treating undruggable diseases,[1−3] such as homozygous familial hypercholesterolemia (HoFH),[4] spinal muscular atrophy (SMA),[5] Duchenne muscular dystrophy (DMD),[6] familial hyperchylomicronemia syndrome (FHCS),[7] and acute myelogenous leukemia (AML).[8] Several oligonucleotide-based drugs have already received approval or are currently undergoing clinical trials. Among them, antisense oligonucleotides (ASOs) have gained significant attention, which could precisely bind to target mRNA, thereby regulating gene expression.[9−11] Combinatorial ASO therapy, which targets multiple mRNA sequences simultaneously, has demonstrated superior efficiency and broader applicability compared to single-target ASO therapy.[12−16] For example, the combination of ASOs targeting the X-linked inhibitor of apoptosis protein (XIAP) and multidrug resistance protein (MRP) has proven effective in simultaneously downregulating these proteins, which significantly reduces drug resistance in AML.[13] Moreover, a combination of different ASOs targeting multiple regions of DMD pre-mRNA has shown a significant increase in therapeutic efficacy, expanding the treatable patient population from 8−13% with single ASO therapy to 40−47%.[14,15] However, the delivery of multiple ASOs in combinatorial therapy has drawn attention to the relevant distribution of different ASOs, which may lead to an unclear ratio of internalized ASOs and affect the reproducibility.

Linear oligonucleotides are known for their short lifetime due to the nucleases in serum or cell plasma. Therefore, chemical modifications such as phosphorothioate (PS) linkages and 2′,4′-constrained 2′-O-ethyl (cEt) have been employed to enhance the stability of linear ASOs.[17−20] However, these modifications raise concerns about potential toxicity and immunogenicity.[18,21] An alternative strategy is the development of circular oligonucleotides with enhanced stability.[22−25] For example, Tang et al. designed a 30 nt c-ODN for the inhibition of miR-21, which showed reduced off-target effects and nonspecific immune stimulation.[26] Additionally, Zhao et al. synthesized a dual-function circular aptamer-ASO chimera (circSApt-NASO), which demonstrated superior efficacy against both SARS-CoV-2 and the Omicron variant.[27] Despite these advantages, circular oligonucleotides face challenges, where the circular structure can introduce tension during the hybridization process, which hinders the efficiency of RNase

Received: May 8, 2025
Revised: June 16, 2025
Accepted: June 17, 2025
Published: July 17, 2025

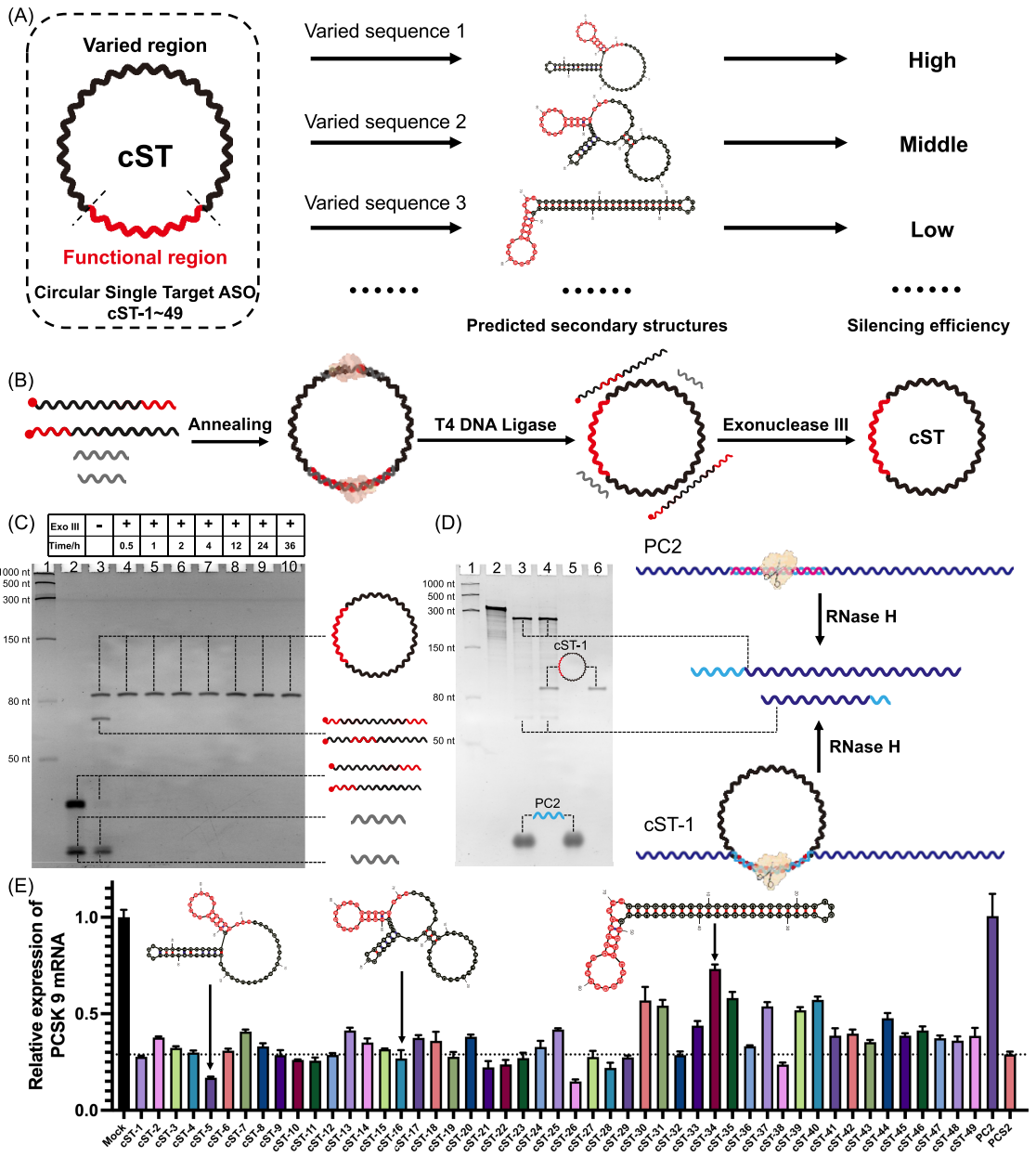

Figure 1. Design, synthesis, and gene silencing performance of multiple circular single-target ASOs (cSTs). (A) Design of cST-1 ∼ 49. (B) Synthesis route of cST-1 ∼ 49. (C) 10% denaturing PAGE analysis of the synthesis and Exo III resistance of cST-1. Lanes 1 to 10: Low-range ssRNA ladder, starting materials, reaction mixture after ligation, and reaction mixture incubation with Exo III for 0.5, 1, 2, 4, 12, 24, and 36 h. (D) 10% denaturing PAGE characterization of in vitro RNase H cleavage of PCSK9 mRNA fragments through cST-1. Lanes 1 to 6: Low-range ssRNA ladder, PCSK9 mRNA fragment, incubation with PC2, and incubation with cST-1, PC2, cST-1. (E) Relative expression of PCSK9 mRNA in HepG2 after treatment with 50 nM cST. The relative PCSK9 mRNA expression was measured through RT-qPCR using GAPDH mRNA as the internal control; at least three independent experiments were performed.

H-mediated cleavage.[23] In principle, a larger circular structure could benefit by alleviating the torsional strain, with greater control over combinatorial ASO therapies. Therefore, the development of large circular ASOs will provide a promising avenue for more effective gene therapy.

In this work, we present a novel strategy that employs programmable, single-stranded circular ASOs for the simultaneous inhibition of multiple genes. A series of large circular ASOs (circASOs) were designed and synthesized, demonstrating a significantly improved gene silencing efficiency compared with their linear counterparts. Notably, unmodified circASOs could achieve a similar silencing efficiency compared to that of chemically modified ASOs. Furthermore, a double-target circASO was also engineered, resulting in the prolonged and more robust cosilencing of two distinct genes. Additionally, the synthesis approach of circASOs enables the precise incorporation of chemical modifications at the single-base level, allowing for further optimization of circASOs. Our methods provide a rational framework for designing circASOs with tailored functional sequences and chemical modifications, offering a versatile tool for the development of multifunctional nucleic acid-based therapies in gene treatment.

https://doi.org/10.1021/jacsau.5c00584
JACS Au 2025, 5, 3555−3564

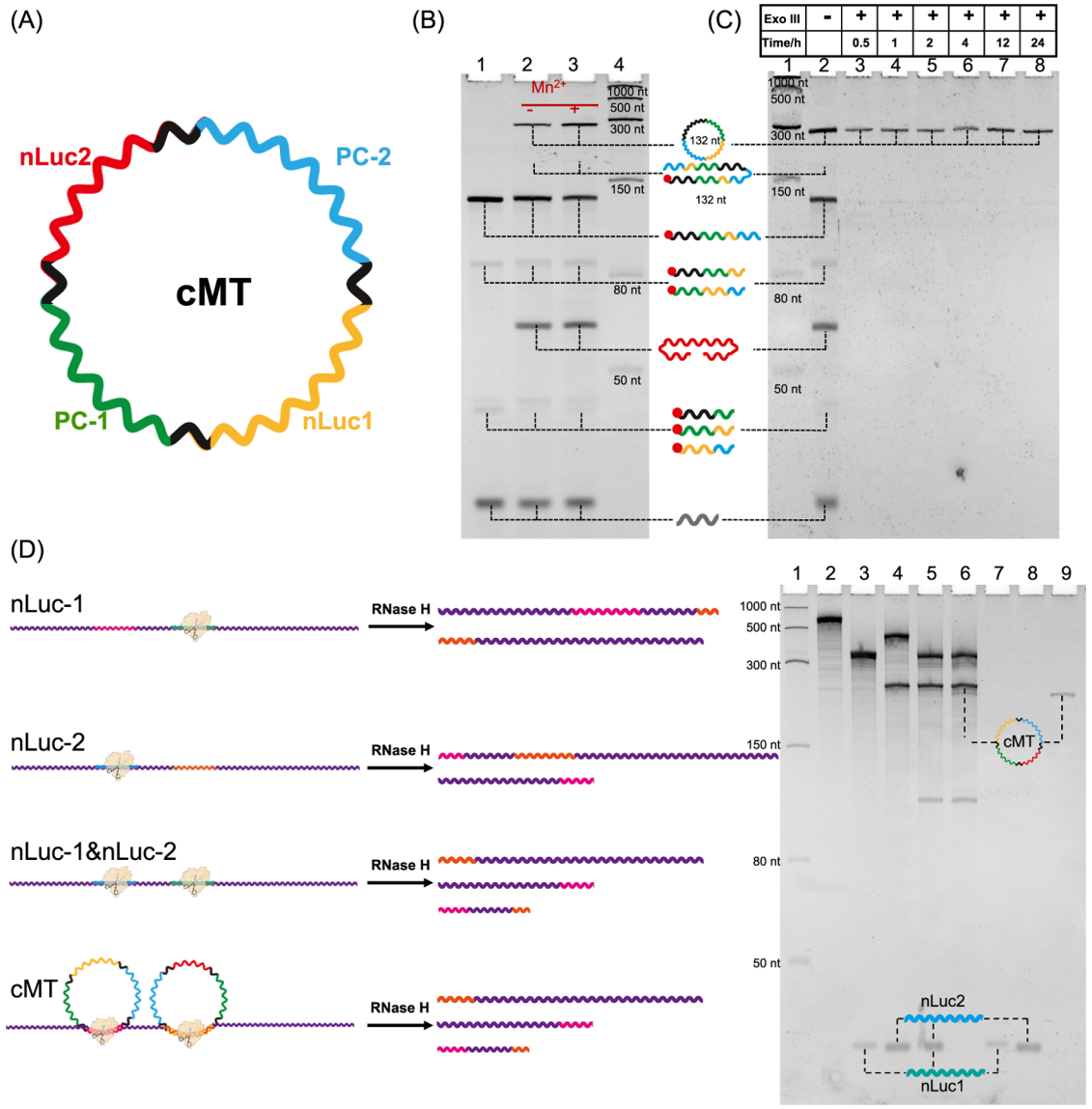

Figure 2. Design and synthesis of the circular multitarget ASO. (A) Design of a single circASO (cMT) for multitarget inhibition. (B) 10% denaturing PAGE characterization of the synthesized circASO. Lanes 1 to 4: Linear ligation; circular ligation without Mn^{2+}; circular ligation with Mn^{2+}; and low-range ssRNA ladder. (C) 10% denaturing PAGE characterization of Exo III resistance of cMT. Lanes 1 to 8: Low-range ssRNA ladder; circular ligation; and incubation of the circular ligation product with Exo III for 0.5, 1, 2, 4, 12, and 24 h. (D) 8% denaturing PAGE characterization of in vitro RNase H-mediated cleavage. Lanes 1 ∼ 9: Low-range ssRNA ladder; nLuc mRNA; incubation with nLuc-1; incubation with nLuc-2; incubation with nLuc-1 and nLuc-2; and incubation with cMT, nLuc-1, nLuc-2, and cMT.

RESULTS AND DISCUSSION

Design and Preparation of Single-Target circASOs

To demonstrate the gene silencing potential of circASOs, a series of single-target circASOs (cST-1 ∼ 49) to proprotein convertase subtilisin/kexin type 9 (PCSK9) were first designed and synthesized. Each cST consists of two regions: a 22-nt functional region that can bind with PCSK9 mRNA and a 49-nt varied region (sequences provided in Table S1) to alleviate the tension during the hybridization between the circASO and mRNA (Figure 1A). The varied region (linker) may interact with the functional region (Figure S1), and different intramolecular interactions could affect the binding affinity and potentially impact the gene silencing efficiency.

The single-target circASOs were synthesized through template-directed ligation, as shown in Figure 1A. Briefly, two oligonucleotides with 5′-phosphate groups were directly circularized by T4 DNA ligase with the assistance of splint DNA. Exonuclease III was then added to remove the linear DNA. Taking cST-1 as an example, as shown in Figure 1B, after ligation, several new bands with lower migration appeared (Lane 2), which can be ascribed to enzymatic ligation. Only one band remained after exonuclease treatment (Lanes 3 to 9), which can be ascribed to cST-1. The circular structure of cST-1 was confirmed through the rolling cycle reaction (RCA). During RCA, phi29 DNA polymerase could produce long single-stranded DNA with a circDNA template, but only double-stranded DNA with a linear template. As shown in Figure S2, the product was accumulated in the sample well when cST-1 was used as the template (Lane 3), and DNA products were no longer observed when linear DNA was used as the template (Lane 5), which confirmed the circular structure of cST-1. Moreover, the MALDI-TOF result (Figure

https://doi.org/10.1021/jacsau.5c00584
JACS Au 2025, 5, 3555−3564

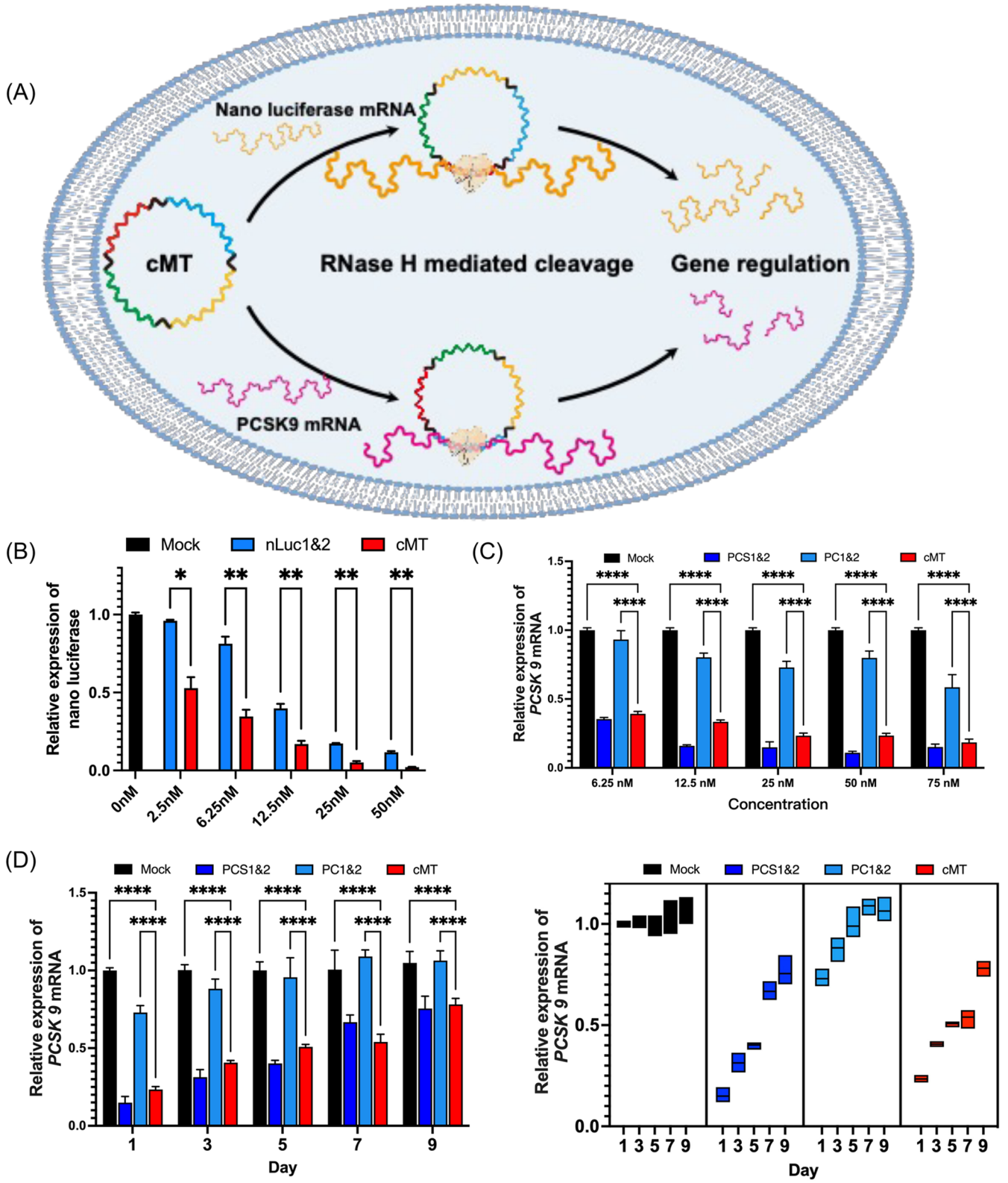

Figure 3. Designed cMT reduced target RNA via RNase H degradation in HepG2. (A) Simultaneous inhibition of PCSK9 mRNA and nanoluciferase mRNA through cMT. (B) Reduction of nanoluciferase expression by cMT in HepG2 cells. (C) Reduction of PCSK9 mRNA by cMT in HepG2 cells. (D) Long-term efficacy of cMT in reducing the PCSK9 mRNA level. The relative PCSK9 mRNA expression was measured through RT-qPCR using GAPDH mRNA as the internal control; at least three independent experiments were performed, and multiple comparisons were performed using one-way ANOVA with Tukey's test. *$P < 0.05$, **$P < 0.01$, ***$P < 0.001$, and ****$P < 0.0001$.

S3) showed a single peak at 21,811 g/mol, which was consistent with the theoretical molecular weight (21,812 g/mol). Similarly, cST-2 to cST-49 were obtained through the same route, and the clear bands shown in Figure S4 indicated

https://doi.org/10.1021/jacsau.5c00584
JACS Au 2025, 5, 3555−3564

the successful synthesis of circASOs. Taken together, the splint ligation and exonuclease digestion strategy could be used for the programmable synthesis of circASOs.

Silencing of the PCSK9 Gene through Single-Target circASOs

The RNase H-mediated cleavage of RNA is essential for the function of the ASO, and therefore, we first tested the in vitro RNase H-mediated mRNA cleavage through the circASO. As shown in Figure 1C, 1 h after the incubation, cST-1 (Lane 4) had successfully cleaved PCSK9 mRNA (the sequence is shown in Table S8) into two fragments as PC2 (Lane 3), which suggested that the circular structure did not affect the cleavage. For further evaluation of the gene silencing efficiency of cST and the effect of the secondary structure of cST, cST-1 ∼ 49 was then transfected into HepG2 cells, which are known for their high expression levels of PCSK9. After 24 h, the relative expression of PCSK9 mRNA was measured through RT-qPCR. As shown in Figure 1E, all circASOs demonstrated a higher gene silencing efficiency compared with unmodified ASOs. Notably, some circASOs, such as cST-5 and cST-26, exhibited an even greater silencing efficiency than chemically modified ASOs (a gapmer design ASO with PS and cEt modifications; the sequence is provided in Table S2).

Considering that the intramolecular interactions within circASOs may impact the gene silencing efficiency through either affecting the binding affinity or the RNase H cleavage activity, the secondary structures of cST-1 ∼ 49 were further predicted by mFold for the investigation of the structure−activity relationship. As shown in Figure S1, no interactions between functional and linker regions in cST-5 and cST-26 were predicted. Instead, their link regions performed some tandem weak interactions, which may synergistically enhance the kinetic stability of the intramolecular interactions.[28] However, the linker regions were predicted with certain structures such as cST-34 and cST-35, which could increase the ring tension of cST and reduce the binding affinity to corresponding mRNA. Taken together, introducing linker regions into the circASO not only relieved tension during DNA-RNA hybridization but also offered greater design flexibility for circASOs. By rationally designing their sequences, unmodified circASOs can achieve a similar or even higher efficiency in comparison to chemically modified linear ASOs.

Design and Synthesis of Multitarget circASOs

After demonstrating the superior single-targeted gene silencing capability of circASOs, we designed a model system to validate the simultaneous inhibition of multiple genes. As shown in Figure 2A, a 132-nt circASO (cMT; sequences are shown in Table S3) containing four different ASO sequences (functional regions) was prepared. Two functional regions were designed to target PCSK9 mRNA (PC1 & PC2), while the other two targeted nanoluciferase mRNA (nLuc-1 and nLuc-2). To minimize potential steric hindrance effects, four nonfunctional linkers (black) were introduced between each functional ASO region. The sequences of the linkers were optimized based on the predicted structure, and the structure of the optimized cMT is shown in Figure S5. It can be observed that there are no cross-talk interactions between functional regions and linkers, and a lack of strong intramolecular interactions is also observed. To facilitate the formation of the circular structure, a rapid synthetic route was developed, as illustrated in Figure S6. Initially, several short DNA fragments were ligated with splint strands to form a linear intermediate (Figure 2B, Lane 1), which was then cyclized by CircLigase (Figure 2B, Lanes 2 and 3).[29,30] Notably, cMT was successfully obtained in up to 50% yield in the presence of Mn^{2+} (Figure 2B, Lane 3). After exonuclease digestion to remove excess linear fragments, the circASO was purified through ethanol precipitation and ultrafiltration.

The circular structure of cMT was also confirmed through exonuclease digestion and rolling circle amplification (RCA). As illustrated in Figure 2C, under the incubation with exonuclease III, the band corresponding to cMT remained, while the linear DNA gradually disappeared with increased incubation time. Moreover, the product was accumulated in the sample well after the RCA reaction (Figure S7, Lane 3), which confirmed the circular structure of cMT. Furthermore, the MALDI-TOF result (Figure S8) revealed a single peak at 40,744 g/mol, corresponding to monomeric circular DNA (with a calculated mass of 40,745 g/mol). These results demonstrated that multitarget cMT was successfully synthesized.

Multitarget RNase H-Mediated Cleavage of mRNA

In our design, cMT could target different regions of nanoluciferase mRNA and generate different fragments, respectively. For the verification of the multitarget cleavage potential of the circASO, cMT was first incubated with nLuc mRNA (the sequence is shown in Table S8) in the presence of RNase H. As shown in Figure 2D, nLuc mRNA was cleaved into three fragments (Lane 6) when incubated with cMT, which was consistent with the molecular design. In contrast, the single ASO could only cleave the mRNA into two fragments (Lanes 3 and 4). Additionally, the incubation with the mixture of nLuc-1 and nLuc-2 (Lane 5) resulted in the same fragments as our cMT. The same result was also observed when the circASO was incubated with PCSK9 mRNA (Figure S9). Taken together, the in vitro cleavage suggested that the different functional regions in cMT could separately act as ASOs and cleave mRNA.

Coinhibition of Nanoluciferase and PCSK9 Using cMT

Next, the multigene silencing potential of cMT was investigated (Figure 3A). cMT was transfected into a model cell line, which could express both nanoluciferase and PCSK9 mRNA simultaneously. As shown in Figure 3B,C, the expressions of both of the target mRNAs were decreased with the increased cMT concentrations. At 12.5 nM, an 83.0% inhibition efficiency (inhibition efficiency = 100% relative expression level compared to mock) against exogenous nanoLuc and a 66.5% inhibition efficiency of endogenous PCSK9 mRNA were observed. However, the inhibition efficiency of PCSK9 was only 19.7% when the mixture of two unmodified linear ASOs (PC1 & PC2; sequences are shown in Table S2) was used, and the inhibition efficiency of nLuc was only 60.2% when the mixture of two unmodified linear ASOs (nLuc-1 & nLuc-2; sequences are shown in Table S2) was used at the same condition. Moreover, based on the silencing effect of nanoluciferase mRNA shown in Figure 3B, the quantitative analysis indicated that the circASO had an IC50 value of 3 nM, while the unmodified linear ASO had an IC50 value of 11.27 nM. Notably, the inhibition efficiency of PCSK9 mRNA under the treatment of cMT was significantly higher than those of PC1 & PC2, demonstrating the superior inhibitory efficacy of the unmodified circASO. Especially, cMT even achieved comparable inhibitory effectiveness to the combination of two chemically modified linear ASOs (PCS1

https://doi.org/10.1021/jacsau.5c00584
JACS Au 2025, 5, 3555−3564

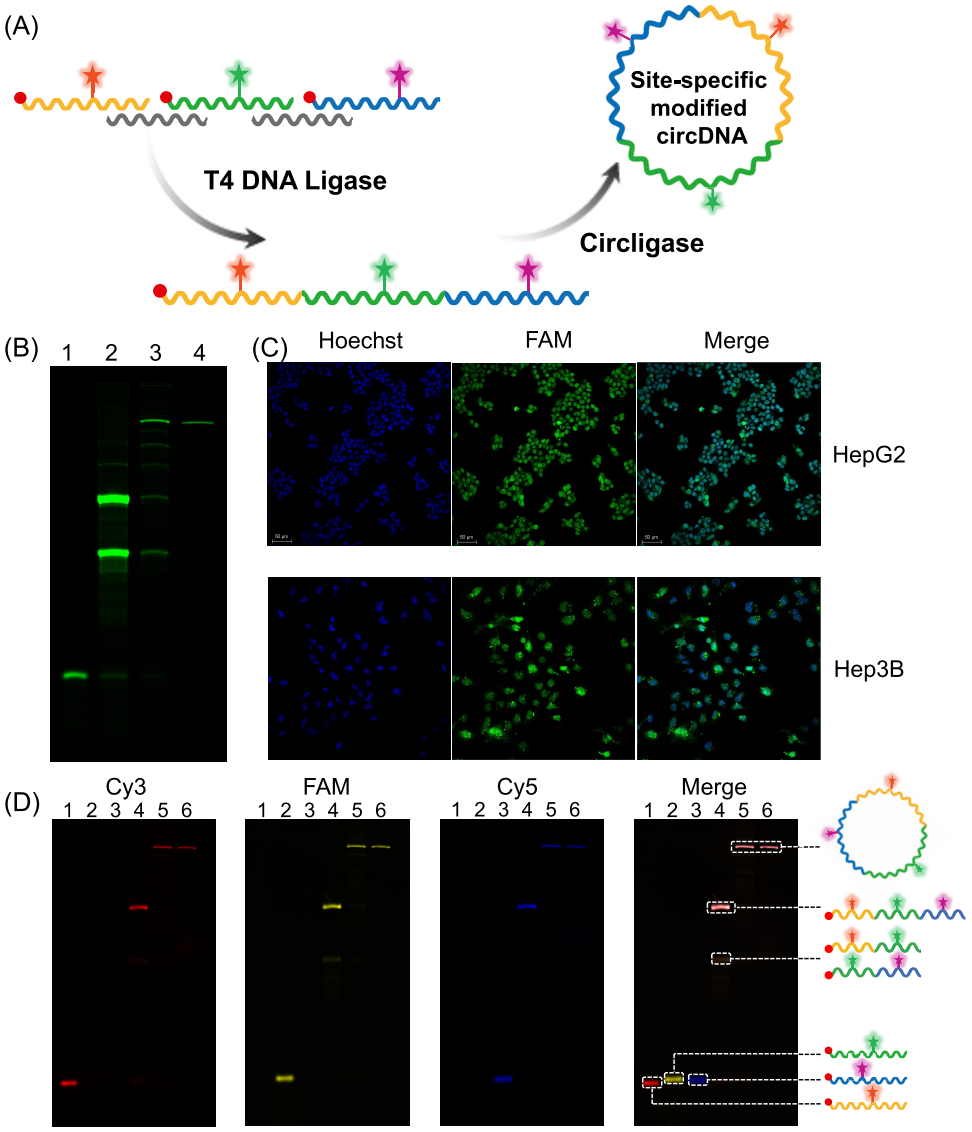

Figure 4. Synthesis and subcellular distribution of the site-specific modified circASO. (A) Synthesis route of the site-specific modified circASO. (B) Synthesis of 67FAM-cMT. Lanes 1 ∼ 4: ASO-2-FAM; the crude product after linear ligation; the crude product after circular ligation; and the final product after Exo III digestion. (C) Laser scanning confocal microscopy images of Hep3B and HepG2 transfected with 67FAM-cMT; the nucleus was stained with Hoechst. (D) 10% denaturing PAGE characterization of the synthesis of 17Cy3-67FAM-106Cy5-cMT. Lanes 1 ∼ 3: Cy3/FAM/Cy5-labeled short DNA fragments; Lane 4: the crude product after linear ligation; Lane 5: the crude product after circular ligation; and Lane 6: the final product after Exo III digestion. The sequences of these modified circular DNAs are shown in Table S4.

& PCS2, Table S2). These results demonstrated the remarkable efficacy of unmodified cMT in downregulating both endogenous and exogenous mRNA levels, with its multitarget effect enabling the simultaneous suppression of multiple mRNA targets.

Next, the long-term inhibitory effect of cMT was evaluated. As depicted in Figure 3D, cMT maintained a 50% inhibition efficiency even after 5 days due to its enhanced biostability. In contrast, unmodified PC1 & PC2 exhibited a diminished inhibitory effect of only 10% on the third day, which reached negligible levels after the fifth day. It was also worth noting that the inhibition efficiency of cMT was comparable with chemically modified PCS1 & PCS2 even 9 days after transfection. The similar long-term inhibition of nanoluciferase was observed in Hep3B cells, which showed a higher inhibition efficiency than the unmodified linear ASO even after 5 days (Figure S10). This prolonged gene inhibition may be attributed to the enhanced stability conferred by the circular structure, which allows for the avoidance of the use of chemical modifications.

To demonstrate that the long-term higher gene silencing efficiency of cMT is due to its super biostability, the tolerance of cMT to the exonucleases (Exo I and Exo V), as well as serum (DMEM containing 10% FBS or 50% FBS), was investigated. As shown in Figure S11, after incubation with different media, there was no significant change of the circASO in the migration rate or intensity under all of the conditions. However, its linear DNA (li-300 nt) showed a significant reduced intensity after the treatment with Exo V for 12 h and completely disappeared after incubation with Exo I for 3 h. It was also found that many diffused bands appeared below the li-300 nt band after incubation with 10% FBS for 12 h, and li-300 nt also completely disappeared after 36 h. Under 50% FBS, the li-300 nt band disappeared entirely only after just 6 h. These

https://doi.org/10.1021/jacsau.5c00584
JACS Au 2025, 5, 3555−3564

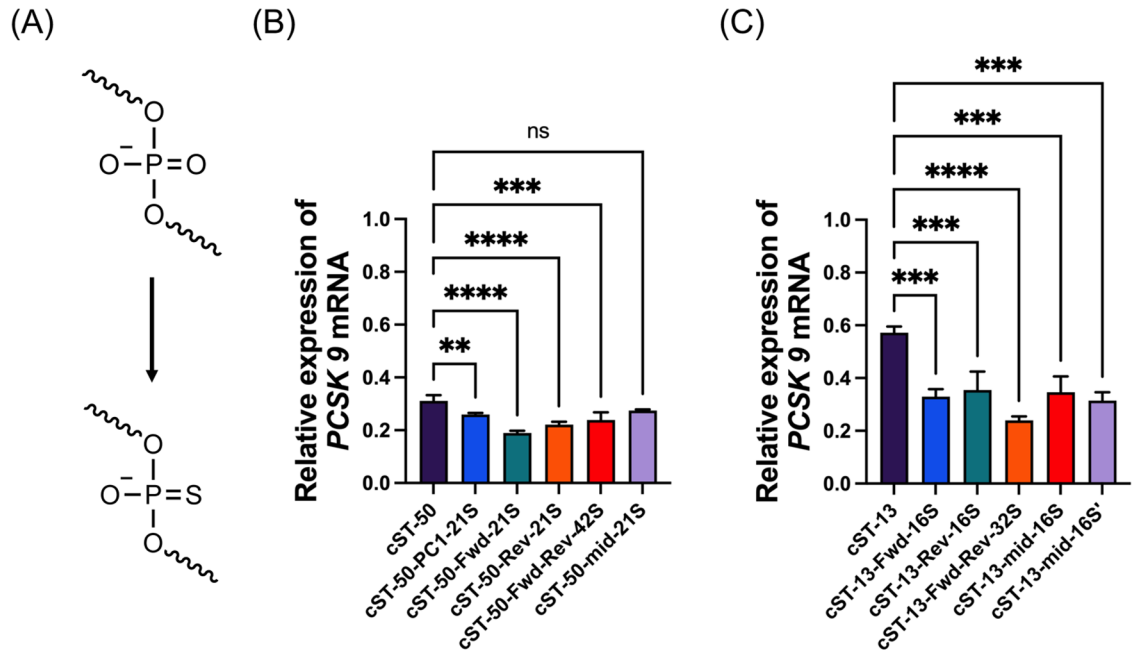

Figure 5. Silencing of PCSK9 mRNA in HepG2 cells using cSTs with different phosphorothioate-modified patterns. (A) Chemical structure of unmodified phosphodiester and phosphorothioate linkages. (B) Silencing of PCSK9 mRNA in HepG2 cells through cST-50, cST-50-PC1-21S, cST-50-Fwd-21S, cST-50-Rev-21S, cST-50-Fwd-Rev-42S, and cST-50-mid-21S. (C) Silencing of PCSK9 mRNA in HepG2 cells through cST-13, cST-13-Fwd-16S, cST-13-Rev-16S, cST-13-Fwd-Rev-32S, cST-13-mid-16S, and cST-13-mid-16S′. The relative PCSK9 mRNA expression was measured through RT-qPCR using GAPDH mRNA as the internal control; at least three independent experiments were performed, and multiple comparisons were performed using one-way ANOVA with Tukey's test. *$P < 0.05$, **$P < 0.01$, ***$P < 0.001$, and ****$P < 0.0001$. The sequences of these modified circular DNAs are shown in Table S5.

results indicated that cMT has higher biostability compared with linear DNA, which could be used for long-term therapy.

As the immunogenicity is a key factor affecting nucleic acid drug development, we tested the immunogenicity of circASOs through the quantification of the mRNA expression level of two kinds of proinflammatory cytokines and chemokines: interferon β (IFN-β) and tumor necrosis factor-α (TNF-α) by RT-qPCR. As shown in Figure S12, the circASOs had low immunogenicity, which is similar to modified linear ASOs, suggesting their potential application in therapy.

Synthesis of Site-Specifically Modified circASOs

Although our strategy eliminated the reliance on the chemical modifications, it is also compatible with various commercially available modifications at a single-base resolution. Principally, different chemical modifications could be site-specifically incorporated into short DNA fragments through solid-phase synthesis and further transferred to the circASO (Figure 4A). A series of circASOs with site-specific single modification and continuous or discontinuous multiple modifications were synthesized for further verification. First, a circASO (67FAM-cMT) with a precisely single-site modification (FAM at T67) was designed as a model system. As shown in Figure 4B, after a standard synthesis procedure and exonuclease digestion, the band corresponding to 67FAM-cMT could be observed under the FAM channel (Figure 4B lane 4). Such a fluorophore-labeled circASO has also facilitated the study of the subcellular distribution. As shown in Figure 4C, 24 h after the transfection to HepG2 and Hep3B, 67FAM-cMT (Green) was localized in both the cytoplasm and the nucleus (Blue) in both cell lines, which was same as the previously reported therapeutic oligonucleotides.

Additionally, combined modifications could also be introduced at a single-base resolution at the same time. Three fluorophores were subsequently chosen and incorporated into 17Cy3-67FAM-106Cy5-cMT (Cy3 at T17, FAM at T67 and Cy5 at T106). As shown in Figure 4D, after linear ligation (Lane 4), circular ligation (Lane 5), and exonuclease III digestion (Lane 6), the bands corresponding to the circular product could be visualized in all fluorescent channels. In addition to fluorophores, the lipophilic 2′-O-hexadecyl (at A20, 20C16-30FAM-cMT) and carbohydrate 2′-O-GalNAc (C18, G19, and A20, $GalNAc_3$-30FAM-cMT) modifications were also successfully introduced, which may facilitate the free uptake of cMT in vivo[31,32] (Figure S13). It is worth noting that these modifications only had a minimal impact on the yield of cMT. These results demonstrated the potential of our ligation method in constructing site-specific chemically modified circDNA structures, which provides a valuable platform for investigation of the functional implications and applications of modified circASOs.

The continuous phosphorothioate linkages could also be introduced into different regions of circASOs with our strategy. Two 71 nt circASOs, cST-50, and cST-13 were chosen as examples, which contain a single functional region PC1 or PC2, respectively. The phosphorothioate-modified patterns are shown in Figure S14 and the silencing efficiency was measured in HepG2. As shown in Figure 5B, the treatment of cST-50-Fwd-21S could reduce the expression of PCSK9 mRNA by 81%, while unmodified cST-50 could reduce the expression by only 69%. Similarly, cST-13-Fwd-Rev-32S showed a 76% reduction, while unmodified cST-13 only showed a 43% reduction. It was also worth noting that even the phosphorothioate modification was not on the functional region; the performance of the circASO could be improved,

https://doi.org/10.1021/jacsau.5c00584
JACS Au 2025, 5, 3555−3564

which indicated that this improvement was not due to the increase of the stability of the functional region. We proposed that this phenomenon is due to the phosphorothioate modification on the circASO binding with some proteins inside the cell, thereby altering its intracellular distribution and enhancing its gene knockdown efficacy. The silencing efficiency in different modification patterns suggested that the site-specific modifications play an important role in the function of circASOs. Thus, all of these results indicated that the efficiency of circASOs could be improved through either structure optimization or site-specific modifications.

CONCLUSIONS

In summary, we proposed the use of circular single-stranded DNA as ASOs for multitarget gene therapy. To circumvent the impact of intramolecular tension during mRNA binding, a nonfunctional region was introduced into the circASO. The single-target circASOs (cSTs) with the same target sequence but different nonfunctional regions demonstrated that the nonfunctional sequence can influence intramolecular interactions, thereby affecting the efficacy of the ASO. Importantly, some of the unmodified cSTs could achieve an inhibition efficiency comparable to third-generation ASOs. Furthermore, we designed a circASO (cMT) capable of simultaneously suppressing the expression of both nLuc and PCSK9 genes. By the introduction of linker sequences between functional regions, each functional region could exert its effect independently. Compared with the use of mixtures of short-chain ASOs, cMT achieved more prolonged simultaneous inhibition of multiple genes in cells, which has been attributed to the higher stability against exonucleases. Meanwhile, our strategy could tolerate numerous chemical modifications, which will further improve the gene silencing efficiency. And based on these site-specific modifications, the detailed mechanism of circASOs such as the endosomal escape behavior and nuclear enrichment could be investigated in the future, which would be beneficial to the further design and development of circASOs. Moreover, our synthetic method for circASOs demonstrated robustness and yielded homogeneous products, indicating its potential for treating diseases like hyperlipidemia. Given the larger quantities required for animal trials, it is necessary to further refine the purification process by employing scalable techniques, such as high-performance liquid chromatography (HPLC) for in vivo validation. Despite the ASO, other functional oligonucleotides such as aptamers[24] and DNAzymes[33,34] could also be integrated into circDNA, which could broaden the application of the circDNA in gene regulation. Although the introduction could cause potential off-target hybridization between the circASO and nontarget mRNA, the activity of RNase H-mediated RNA cleavage needs a perfect complementary, reducing off-target gene silencing likelihood. Besides, due to the tolerance of our methods to various chemical modifications, they could be further introduced to reduce the potential off-target effects. Taken together, the strategy we proposed here has universality in terms of the sequence, size, and modifications, and our results revealed great promise of the application of modified circDNA as novel tools for multigene regulation research and in future molecular therapy.

ASSOCIATED CONTENT

Supporting Information

The Supporting Information is available free of charge at https://pubs.acs.org/doi/10.1021/jacsau.5c00584.

Experimental details, materials, methods, sequence information, and some experimental results (PDF)

AUTHOR INFORMATION

Corresponding Authors

Yuanchen Dong − *CAS Key Laboratory of Colloid, Interface and Chemical Thermodynamics, Institute of Chemistry, Chinese Academy of Sciences, Beijing 100190, China; University of Chinese Academy of Sciences, Beijing 100049, China;* orcid.org/0000-0002-0653-7760; Email: dongyc@iccas.ac.cn

Dongsheng Liu − *Engineering Research Center of Advanced Rare Earth Materials (Ministry of Education), Department of Chemistry, Tsinghua University, Beijing 100084, China; Department of Applied Biology and Chemical Technology, The Hong Kong Polytechnic University, Kowloon, Hong Kong 999077, China; The Hong Kong Polytechnic University Shenzhen Research Institute, Shenzhen 518057, China;* orcid.org/0000-0002-2583-818X; Email: dongsheng.liu@polyu.edu.hk

Authors

Yufan Pan − *Engineering Research Center of Advanced Rare Earth Materials (Ministry of Education), Department of Chemistry, Tsinghua University, Beijing 100084, China*

Xin Li − *Engineering Research Center of Advanced Rare Earth Materials (Ministry of Education), Department of Chemistry, Tsinghua University, Beijing 100084, China*

Chenyou Zhu − *Engineering Research Center of Advanced Rare Earth Materials (Ministry of Education), Department of Chemistry, Tsinghua University, Beijing 100084, China*

Mingyan Wang − *Beijing SupraCirc Biotechnology Co., Ltd, Beijing 100195, China*

Yuanyuan Wu − *Beijing SupraCirc Biotechnology Co., Ltd, Beijing 100195, China*

Rui Xu − *Engineering Research Center of Advanced Rare Earth Materials (Ministry of Education), Department of Chemistry, Tsinghua University, Beijing 100084, China*

Jun Wu − *CAS Key Laboratory of Colloid, Interface and Chemical Thermodynamics, Institute of Chemistry, Chinese Academy of Sciences, Beijing 100190, China; University of Chinese Academy of Sciences, Beijing 100049, China*

Ruofan Chen − *Engineering Research Center of Advanced Rare Earth Materials (Ministry of Education), Department of Chemistry, Tsinghua University, Beijing 100084, China;* orcid.org/0000-0001-5954-8765

Yifan Jiang − *Engineering Research Center of Advanced Rare Earth Materials (Ministry of Education), Department of Chemistry, Tsinghua University, Beijing 100084, China*

Baolei Tian − *Beijing SupraCirc Biotechnology Co., Ltd, Beijing 100195, China*

Complete contact information is available at: https://pubs.acs.org/10.1021/jacsau.5c00584

Author Contributions

[▽]Y.P. and X.L. contributed equally.

https://doi.org/10.1021/jacsau.5c00584
JACS Au 2025, 5, 3555−3564

Notes

The authors declare no competing financial interest.

■ ACKNOWLEDGMENTS

This work was supported by the National Basic Research Plan of China (2023YFA0915201, 2024YFA1308500), the Beijing Municipal Science & Technology Commission (Z231100007223003), the Beijing Natural Science Foundation (JQ24007), and the National Natural Science Foundation of China (22477122).

■ REFERENCES

(1) Crooke, S. T.; Baker, B. F.; Crooke, R. M.; Liang, X. Antisense Technology: An Overview and Prospectus. *Nat. Rev. Drug Discovery* **2021**, *20* (6), 427−453.
(2) Jadhav, V.; Vaishnaw, A.; Fitzgerald, K.; Maier, M. A. RNA. Interference in the Era of Nucleic Acid Therapeutics. *Nat. Biotechnol.* **2024**, *42* (3), 394−405.
(3) Xu, R.; Li, Y.; Zhu, C.; Liu, D.; Yang, Y. R. Cellular Ingestible DNA Nanostructures for Biomedical Applications. *Adv. Nanobiomed Res.* **2023**, *3* (1), No. 2200119.
(4) Raal, F. J.; Santos, R. D.; Blom, D. J.; Marais, A. D.; Charng, M.-J.; Cromwell, W. C.; Lachmann, R. H.; Gaudet, D.; Tan, J. L.; Chasan-Taber, S.; Tribble, D. L.; Flaim, J. D.; Crooke, S. T. Mipomersen, an Apolipoprotein B Synthesis Inhibitor, for Lowering of LDL Cholesterol Concentrations in Patients with Homozygous Familial Hypercholesterolaemia: A Randomised, Double-Blind, Placebo-Controlled Trial. *Lancet* **2010**, *375* (9719), 998−1006.
(5) Finkel, R. S.; Mercuri, E.; Darras, B. T.; Connolly, A. M.; Kuntz, N. L.; Kirschner, J.; Chiriboga, C. A.; Saito, K.; Servais, L.; Tizzano, E.; Topaloglu, H.; Tulinius, M.; Montes, J.; Glanzman, A. M.; Bishop, K.; Zhong, Z. J.; Gheuens, S.; Bennett, C. F.; Schneider, E.; Farwell, W.; De Vivo, D. C. Nusinersen versus Sham Control in Infantile-Onset Spinal Muscular Atrophy. *N. Engl. J. Med.* **2017**, *377* (18), 1723−1732.
(6) Dhillon, S. Viltolarsen: First Approval. *Drugs* **2020**, *80* (10), 1027−1031.
(7) Stroes, E. S. G.; Alexander, V. J.; Karwatowska-Prokopczuk, E.; Hegele, R. A.; Arca, M.; Ballantyne, C. M.; Soran, H.; Prohaska, T. A.; Xia, S.; Ginsberg, H. N.; Witztum, J. L.; Tsimikas, S. Olezarsen, Acute Pancreatitis, and Familial Chylomicronemia Syndrome. *N. Engl. J. Med.* **2024**, *390* (19), 1781−1792.
(8) Macečková, D.; Vaňková, L.; Bufka, J.; Hošek, P.; Moravec, J.; Pitule, P. Antisense Oligonucleotides as a Targeted Therapeutic Approach in Model of Acute Myeloid Leukemia. *Mol. Biol. Rep.* **2024**, *52* (1), No. 57.
(9) Yuan, W.; Cheng, J.; Zhu, C.; Dong, G.; Zhao, X.; Meng, S.; Liu, D.; Dong, Y. Preparing Liposomes through Frame Guided Assembly with High-Loading Functional Nucleic Acids. *Nanoscale* **2023**, *15* (23), 9946−9953.
(10) Wei, X.; Li, Y.; Cheng, X.; Wen, Y.; Yuan, W.; Chen, R.; Meng, S.; Lu, X.; Yu, Z.; Xu, L.; Liu, D.; Dong, Y. Increase Nebulization Stability of Lipid Nanoparticles by Integrating a DNA Supramolecular Hydrogel. *ACS Macro Lett.* **2023**, *12* (6), 745−750.
(11) Zhang, Y.; Hou, X.; Piao, J.; Yuan, W.; Zhou, B.; Zhao, X.; Hao, Z.; Zhuang, Y.; Xu, L.; Dong, Y.; Liu, D. Delivery and Controllable Release of Anti-Sense DNA Based on Frame-Guided Assembly Strategy. *Eur. Polym. J.* **2022**, *173*, No. 111187.
(12) Li, Y.; Li, J.; Wang, J.; Lynch, D. R.; Shen, X.; Corey, D. R.; Parekh, D.; Bhat, B.; Woo, C.; Cherry, J. J.; Napierala, J. S.; Napierala, M. Targeting 3′ and 5′ Untranslated Regions with Antisense Oligonucleotides to Stabilize Frataxin mRNA and Increase Protein Expression. *Nucleic Acids Res.* **2021**, *49* (20), 11560−11574.
(13) Wang, X.; Wang, C.; Qin, Y.; Yan, S.; Gao, Y. Simultaneous Suppression of Multidrug Resistance and Antiapoptotic Cellular Defense Induces Apoptosis in Chemoresistant Human Acute Myeloid Leukemia Cells. *Leuk. Res.* **2007**, *31* (7), 989−994.
(14) Lim, K. R. Q.; Woo, S.; Melo, D.; Huang, Y.; Dzierlega, K.; Shah, M. N. A.; Aslesh, T.; Roshmi, R. R.; Echigoya, Y.; Maruyama, R.; Moulton, H. M.; Yokota, T. Development of DG9 Peptide-Conjugated Single- and Multi-Exon Skipping Therapies for the Treatment of Duchenne Muscular Dystrophy. *Proc. Natl. Acad. Sci, U. S. A.* **2022**, *119* (9), No. e2112546119.
(15) Yanagidaira, M.; Yoshioka, K.; Nagata, T.; Nakao, S.; Miyata, K.; Yokota, T. Effects of Combinations of Gapmer Antisense Oligonucleotides on the Target Reduction. *Mol. Biol. Rep.* **2023**, *50* (4), 3539−3546.
(16) Zhou, L.; Bi, J.; Chang, S.; Bai, Z.; Yu, J.; Wang, R.; Li, Z.; Zhang, X.; Chou, J. J.; Pan, L. Self-Assembled Antibody-Oligonucleotide Conjugates for Targeted Delivery of Complementary Antisense Oligonucleotides. *Angew. Chem., Int. Ed.* **2025**, *64* (3), No. e202415272.
(17) Shen, W.; De Hoyos, C. L.; Migawa, M. T.; Vickers, T. A.; Sun, H.; Low, A.; Bell, T. A.; Rahdar, M.; Mukhopadhyay, S.; Hart, C. E.; Bell, M.; Riney, S.; Murray, S. F.; Greenlee, S.; Crooke, R. M.; Liang, X.; Seth, P. P.; Crooke, S. T. Chemical Modification of PS-ASO Therapeutics Reduces Cellular Protein-Binding and Improves the Therapeutic Index. *Nat. Biotechnol.* **2019**, *37* (6), 640−650.
(18) Anderson, B. A.; Freestone, G. C.; Low, A.; De-Hoyos, C. L.; Drury, W. J., III; Østergaard, M. E.; Migawa, M. T.; Fazio, M.; Wan, W. B.; Berdeja, A.; Scandalis, E.; Burel, S. A.; Vickers, T. A.; Crooke, S. T.; Swayze, E. E.; Liang, X.; Seth, P. P. Towards next Generation Antisense Oligonucleotides: Mesylphosphoramidate Modification Improves Therapeutic Index and Duration of Effect of Gapmer Antisense Oligonucleotides. *Nucleic Acids Res.* **2021**, *49* (16), 9026−9041.
(19) Roberts, T. C.; Langer, R.; Wood, M. J. A. Advances in Oligonucleotide Drug Delivery. *Nat. Rev. Drug Discovery* **2020**, *19* (10), 673−694.
(20) Lu, M.; Xing, H.; Zheng, A.; Huang, Y.; Liang, X.-J. Overcoming Pharmaceutical Bottlenecks for Nucleic Acid Drug Development. *Acc. Chem. Res.* **2023**, *56* (3), 224−236.
(21) Shi, Y.; Zhen, X.; Zhang, Y.; Li, Y.; Koo, S.; Saiding, Q.; Kong, N.; Liu, G.; Chen, W.; Tao, W. Chemically Modified Platforms for Better RNA Therapeutics. *Chem. Rev.* **2024**, *124* (3), 929−1033.
(22) Cao, X.; Tang, L.; Song, J. Circular Single-Stranded DNA: Discovery, Biological Effects, and Applications. *ACS Synth. Biol.* **2024**, *13* (4), 1038−1058.
(23) Zhao, X.; Xu, J.; Liang, X.; Wang, Z.; Zhu, Y.; Guo, D.; Wang, J.; Amu, G.; Wang, Q.; Yang, Z.; Tang, X. NQO1-Activatable Circular Antisense Oligonucleotides for Tumor-Cell-Specific Survivin Gene Silencing and Antitumor Therapy. *J. Med. Chem.* **2025**, *68* (4), 4466−4476.
(24) Chen, J.; Chi, H.; Wang, C.; Du, Y.; Wang, Y.; Yang, S.; Jiang, S.; Lv, X.; He, J.; Chen, J.; Fu, T.; Wang, Z.; Cheng, M.; An, K.; Zhang, P.; Tan, W. Programmable Circular Multispecific Aptamer-Drug Engager to Broadly Boost Antitumor Immunity. *J. Am. Chem. Soc.* **2024**, *146* (50), 34311−34323.
(25) Liu, X.; Tong, J.; Li, M.; Li, L.; Cai, W.; Li, J.; Wang, L.; Sun, M. Progress in Application of Cyclic Single-Stranded Nucleic Acids. *J. Biotechnol.* **2024**, *393*, 140−148.
(26) Gubu, A.; Su, W.; Zhao, X.; Zhang, X.; Fan, X.; Wang, J.; Wang, Q.; Tang, X. Circular Antisense Oligonucleotides for Specific RNase-H-Mediated microRNA Inhibition with Reduced Off-Target Effects and Nonspecific Immunostimulation. *J. Med. Chem.* **2021**, *64* (21), 16046−16055.
(27) Yang, G.; Zhang, S.; Song, W.; Bai, X.; Li, L.; Luo, F.; Cheng, Y.; Wang, D.; Wang, Y.; Chen, J.; Zhao, J.; Zhao, Y. Efficient Targeted Delivery of Bifunctional Circular Aptamer-ASO Chimera to Suppress the SARS-CoV-2 Proliferation and Inflammation. *Small* **2023**, *19* (16), No. 2207066.
(28) Li, X.; Dai, X.; Pan, Y.; Sun, Y.; Yang, B.; Chen, K.; Wang, Y.; Xu, J.-F.; Dong, Y.; Yang, Y. R.; Yan, L.-T.; Liu, D. Studies on the Synergistic Effect of Tandem Semi-Stable Complementary Domains on Sequence-Defined DNA Block Copolymers. *J. Am. Chem. Soc.* **2022**, *144* (46), 21267−21277.

https://doi.org/10.1021/jacsau.5c00584
JACS Au 2025, 5, 3555−3564

(29) Shi, J.; Jia, H.; Chen, H.; Wang, X.; Xu, J. F.; Ren, W.; Zhao, J.; Zhou, X.; Dong, Y.; Liu, D. Concentration Insensitive Supramolecular Polymerization Enabled by Kinetically Interlocking Multiple-Units Strategy. *CCS Chem.* **2019**, *1* (3), 296−303.
(30) Li, Q.; Zhang, S.; Li, W.; Ge, Z.; Fan, C.; Gu, H. Programming CircLigase Catalysis for DNA Rings and Topologies. *Anal. Chem.* **2021**, *93* (3), 1801−1810.
(31) Tanowitz, M.; Hettrick, L.; Revenko, A.; Kinberger, G. A.; Prakash, T. P.; Seth, P. P. Asialoglycoprotein Receptor 1 Mediates Productive Uptake of N-Acetylgalactosamine-Conjugated and Unconjugated Phosphorothioate Antisense Oligonucleotides into Liver Hepatocytes. *Nucleic Acids Res.* **2017**, *45* (21), 12388−12400.
(32) Brown, K. M.; Nair, J. K.; Janas, M. M.; Anglero-Rodriguez, Y. I.; Dang, L. T. H.; Peng, H.; Theile, C. S.; Castellanos-Rizaldos, E.; Brown, C.; Foster, D.; Kurz, J.; Allen, J.; Maganti, R.; Li, J.; Matsuda, S.; Stricos, M.; Chickering, T.; Jung, M.; Wassarman, K.; Rollins, J.; Woods, L.; Kelin, A.; Guenther, D. C.; Mobley, M. W.; Petrulis, J.; McDougall, R.; Racie, T.; Bombardier, J.; Cha, D.; Agarwal, S.; Johnson, L.; Jiang, Y.; Lentini, S.; Gilbert, J.; Nguyen, T.; Chigas, S.; LeBlanc, S.; Poreci, U.; Kasper, A.; Rogers, A. B.; Chong, S.; Davis, W.; Sutherland, J. E.; Castoreno, A.; Milstein, S.; Schlegel, M. K.; Zlatev, I.; Charisse, K.; Keating, M.; Manoharan, M.; Fitzgerald, K.; Wu, J.-T.; Maier, M. A.; Jadhav, V. Expanding RNAi Therapeutics to Extrahepatic Tissues with Lipophilic Conjugates. *Nat. Biotechnol.* **2022**, *40* (10), 1500−1508.
(33) Zhao, H.; Yi, D.; Li, L.; Zhao, Y.; Li, M. Modular Weaving DNAzyme in Skeleton of DNA Nanocages for Photoactivatable Catalytic Activity Regulation. *Angew. Chem., Int. Ed.* **2024**, *63* (18), No. e202404064.
(34) Xie, X.; Nan, H.; Peng, J.; Zeng, K.; Wang, H.-H.; Huang, Y.; Nie, Z. Hydrogen Sulfide-Triggered Artificial DNAzyme Switches for Precise Manipulation of Cellular Functions. *Angew. Chem., Int. Ed.* **2024**, *63* (49), No. e202410380.

https://doi.org/10.1021/jacsau.5c00584
JACS Au 2025, 5, 3555−3564